Novel E-Cadherin-mediated Adhesion in Peripheral Nerve: Schwann Cell Architecture Is Stabilized by Autotypic Adherens Junctions

Allison M. Fannon,* Diane L. Sherman,‖ Galina Ilyina-Gragerova,* Peter J. Brophy,‖ Victor L. Friedrich Jr.,*‡ and David R. Colman*‡§

*Brookdale Center for Molecular Biology,‡ The Fishberg Center for Neuroscience, and §The Department of Cell Biology and Anatomy, The Mount Sinai School of Medicine, New York, New York 10029; and ‖Department of Preclinical Veterinary Sciences, University of Edinburgh, Edinburgh EH9 1QH United Kingdom

Abstract. Previous studies (Blank, W. F., M. B. Bunge, and R. P. Bunge. 1974. *Brain Res.* 67:503–518) showed that Schwann cell paranodal membranes were disrupted in calcium free medium suggesting that cadherin mediated mechanisms may operate to maintain the integrity of the paranodal membrane complex. Using antibodies against the fifth extracellular domain of E-cadherin, we now show by confocal laser and electron immunomicroscopy that E-cadherin is a major adhesive glycoprotein in peripheral nervous system Schwann cells. E-Cadherin is not found, however, in compact myelin bilayers. Rather, it is concentrated at the paranodes, in Schmidt-Lanterman incisures, and at the inner and outer loops. At these loci, E-cadherin is associated with subplasmalemmal electron densities that coordinate in register across several cytoplasmic turns of a single Schwann cell. F-Actin and β-catenin, two proteins implicated in cellular signaling, also co-localize to E-cadherin positive sites. These complexes are autotypic adherens-type junctions that are confined to the plasma membrane synthesized by a single Schwann cell; E-cadherin was never observed between two Schwann cells, nor between Schwann cells and the axon. Our findings demonstrate that E-cadherin and its associated proteins are essential components in the architecture of the Schwann cell cytoplasmic channel network, and suggest that this network has specialized functions in addition to those required for myelinogenesis.

SCHWANN cells, which synthesize myelin in the peripheral nervous system (PNS)[1], have a highly specialized architecture consisting of myelin surrounded by a thin, highly convoluted, but continuous cytoplasmic channel network. This network is physiologically active and is organized into several well-defined morphological regions. These include the inner and outer loops, Schmidt-Lanterman incisures and the paranodal channels (Peters et al., 1991). By electron microscopy, the paranodal channels appear to be a series of loops that are often referred to as "paranodal loops." Early in peripheral nerve development Schwann cells align along individual axonal fibers and establish domains that will become the future myelin internodes that segregate nodes of Ranvier. As wrapping of the axon commences, the Schwann cell plasma membrane compacts and circumferential layers of myelin are rapidly laid down. At the end of each internode myelin lamellae terminate in helically coiled paranodal channels that are continuous with the cytoplasm of the Schwann cell soma. Within the internode, compact myelin layers become sequestered into many small "islands" by funnel-shaped spirals of cytoplasm known as Schmidt-Lanterman incisures.

The pseudocrystalline architecture of compact myelin in the PNS is maintained by P_0, an immunoglobulin gene superfamily member with exceptionally strong adhesive properties (D'Urso et al., 1990; Filbin et al., 1990; Doyle and Colman, 1993). It is likely that compact myelin lamellae, once formed, are extremely stable and essentially metabolically inactive. However, the extensive cytoplasmic channel network that borders compact myelin is known to be highly dynamic (Singer and Bryant, 1969; Joe and Angelides, 1992), and it is generally believed that addition and retrieval of biosynthetic components take place at the myelin–cytoplasmic channel interface. The mechanical forces that maintain, and act on and within these channels are not understood, nor are the unique functions of channel subdomains

Address all correspondence to A. Fannon, Brookdale Center for Molecular Biology, Box 1126, The Mount Sinai School of Medicine, One Gustave L. Levy Place, New York, NY 10029. Ph.: (212) 241-5773. Fax: (212) 423-0596.

1. *Abbreviations used in this paper*: E, epithelial; EC, extracellular; GST, glutathione-S-transferase; N, neural; P, placental; PNS, peripheral nervous system.

fully appreciated as yet. Over recent years, it has become apparent that certain well-studied proteins, that in other cell types are known to be involved in cell or membrane motility and the generation of cell shape and polarity are found within the channel network of the Schwann cell. These include tubulin (Peters et al., 1991), actin, and spectrin (Trapp et al., 1989), ankyrin (Kordeli et al., 1990), connexin 32 (Bergoffen et al., 1993), and certain integrins (Einheber et al., 1993).

The structural integrity of Schwann cells, particularly the paranodal loops, has been shown to be sensitive to calcium (Blank et al., 1974). When cultured sensory ganglia were incubated in low calcium medium, lengthening of the node of Ranvier, swelling of the extracellular space between the paranodal loops, and separation and shrinkage of the axon away from the myelin sheath were observed. Over time, dissociation of the junction between the paranodal loops and the axolemma was noted. These changes were reversible upon return to normal calcium concentrations. These data prompted us to examine whether cadherins might be involved in the formation and maintenance of the nodal architecture.

The cadherins are a superfamily of calcium dependent adhesion proteins that function in cell recognition and segregation, morphogenetic regulation, and tumor suppression (for reviews see Magee and Buxton, 1991; Takeichi, 1991; Geiger and Ayalon, 1992; Grunwald, 1993). The classical cadherins are the most well studied and include N-cadherin (neural cadherin, ACAM), E-cadherin (epithelial cadherin, uvomorulin, arc LCAM), and P-cadherin (placental cadherin). They have a common primary structure that consists of an NH_2-terminal extracellular domain, a short transmembrane domain and a highly conserved COOH-terminal cytoplasmic domain which is responsible for interaction with cytoplasmic proteins (Nagafuchi and Takeichi, 1988) and subsequent stabilization of junctional complexes (Näthke et al., 1994). The extracellular domain can be divided into five regions referred to as extracellular regions 1 (EC1) to EC5 (Grunwald, 1993). EC1 through EC4 are highly homologous to each other and contain putative calcium binding sequences. EC5 is the least homologous region and had been distinguished from the other EC regions as a premembrane domain (Berndorff et al., 1994) or the extracellular anchor domain (Magee and Buxton, 1991).

Using highly specific antibodies that we raised against EC5 of E-cadherin, we now demonstrate by confocal laser and electron immunomicroscopy that E-cadherin is a major adhesive glycoprotein restricted to noncompacted plasma membranes within myelin internodes in peripheral nerve. E-Cadherin is excluded from myelin and therefore does not take an active role in the compaction or adhesion of these membranes. Most importantly, E-cadherin is not detected in the axonal membrane, and thus in the PNS, E-cadherin uniquely mediates adhesion between plasma membranes elaborated by a single cell. E-cadherin is concentrated at the inner and outer loops, and in Schmidt-Lanterman incisures, but is most intensely distributed in plasma membranes associated with electron-dense cytoplasmic plaques that are in register across paranodal loops. We identify these complexes as helically arranged adherens-type junctions that are autotypic; that is, they link plasma membrane wraps of the same Schwann cell. Our findings reveal that cytoplasmic regions in the Schwann cell are actively self-adherent and structurally maintained at least in part by an E-cadherin–mediated adhesion mechanism.

Materials and Methods

Antibodies

For neurofilament immunolabeling, a mixture of two mouse monoclonal antibodies, SMI 32 and RMO108, was used. SMI32 (Sternberger Monoclonals Inc., Baltimore, MD) recognizes a nonphosphorylated epitope in high neurofilament protein, and RMO108 (Lee et al., 1987) recognizes a phosphorylated epitope in rat middle neurofilament protein. MAG antibodies (Mouse anti-MAG clone 513; Boehringer-Mannheim Biochemicals, Indianapolis, IN) were used for double-labeling experiments. β-Catenin antibodies (mouse anti–β-catenin), used for immunocytochemistry, were a gift of Karen Knudsen (Lankenau Medical Research Center, Wynnewood, PA). Phalloidin-rhodamine (0.33 μM; Molecular Probes, Eugene, OR) was used to localize F-actin, and diD (1-1'-dioctadecyl-3,3,3'3,3'-tetramethylindodicarbocyanine, Molecular Probes) was used at 25 μm/ml to label membranes. Commercially available E-cadherin antibodies, DECMA-1 (rat anti–uvomorulin) and ECCD-2 (rat anti–E-cadherin) were purchased from Sigma Chem. Co., St. Louis, MO and Zymed Labs Inc. (S. San Francisco, CA), respectively. N-cadherin antibodies (mouse anti-ACAM, clone GC-4) and mouse anti–vinculin (clone hVIN-1) were purchased from Sigma Chem. Co. Rabbit anti–α- and β-catenin, were a gift of Barry Gumbiner (Memorial Sloan-Kettering Cancer Center, New York, NY).

Preparation of EcadEC5 Antibodies

To produce an E-cadherin specific antibody, E-cadherin cDNA was RT-PCR amplified from total RNA which had been purified from adult mouse brain (strain B6D2 F_1) using RNAzol B (Cinna/Biotecx, Houston, TX). A 300-bp Bam HI fragment (nucleotides 1920-2212; Nagafuchi et al., 1987), which contained most of the fifth extracellular region and a small portion of the transmembrane domain of mouse E cadherin (see Fig. 1 *A*), was purified and subcloned into the glutathione-S-transferase (GST) fusion protein bacterial expression vector, pGEX 3X (Pharmacia, Piscataway, NJ). The fusion protein, GST-EcadEC5, was purified from bacterial lysates by affinity chromatography using glutathione-agarose (Sigma Chem. Co.). GST-EcadEC5 was digested with Factor Xa (Boehringer-Mannheim Biochemicals) to generate an EcadEC5 fragment which was then purified using Pharmacia Mono Q FPLC anion exchange chromatography. Rabbits were immunized with EcadEC5 at Pocono Rabbit Farms (Canadensis, PA). To generate EcadEC5 antibodies, a primary injection (50 μl) of purified EcadEC5 (100 μg) emulsified in Freund's complete adjuvant was injected into the popliteal lymph nodes of rabbits. Boosts, consisting of EcadEC5 (50 μg) emulsified in Freund's incomplete adjuvant were administered by subcutaneous injection on days 7, 14, and 28, and every fourth week thereafter. Serum was collected weekly. High titer antiserum (>1:5,000 dilution on Western blots of fusion protein) was obtained after the third boost. Anti-EcadEC5 was affinity purified (Harlow and Lane, 1988) using GST-EcadEC5–conjugated Sepharose columns.

SDS-PAGE and Western Blotting

Freshly dissected adult mouse (strain B6D2 F_1) or rat (Sprague Dawley) sciatic nerves were homogenized in 5% SDS, 200 mM DTT, aprotinin (1 μg/ml), leupeptin (10 μg/ml), 1 mM pefabloc SC, and pepstatin (10 μg/ml) (Boehringer-Mannheim Biochemicals). The homogenates were briefly centrifuged for 1 min at 14,000 rpm to remove insoluble material, diluted 1:1 with SDS-PAGE sample buffer and boiled for 5 min. Sciatic nerve homogenates were separated by SDS-PAGE using 7.5% polyacrylamide gels and transferred to nitrocellulose. An osmotically shocked membrane fraction was prepared from two week old Wistar rat trigeminal or sciatic nerves as previously described (Gillespie et al., 1994), separated by SDS-PAGE on 5–17% gradient polyacrylamide gels and transferred to nitrocellulose. For immunodetection, the nitrocellulose was blocked with 5% nonfat milk and incubated with primary antibodies. Anti-EcadEC5 was used at 1:1,000 dilution (serum) or at 2.5 μg/ml (affinity purified). Commercial primary antibodies were diluted according to the manufacturers' recommendations. For detection, the blots were incubated with alkaline phosphatase (Sigma Chem. Co.) or peroxidase (Jackson ImmunoResearch Laboratories, Inc., West Grove, PA) conjugated secondary antibodies and developed with nitro

blue tetrazolium and 5-bromo-4-chloro-3-indolyl phosphate (Sigma Chem. Co.) or chemiluminescence (Amersham Corp.). Relative molecular weights for E-cadherin and the catenins were calculated using broad range molecular weight standards (Bio-Rad Laboratories, Cambridge, MA).

Immunoprecipitations

Freshly dissected kidney and sciatic nerve from adult mice (Strain B6D2 F_1), and human brain tissue were homogenized in ice cold 2% SDS, TBS (20 mM Tris, pH 7.5, 150 mM NaCl), aprotinin (1 μg/ml), leupeptin (10 μg/ml), 1 mM pefabloc SC, and pepstatin (10 μg/ml), and boiled for 5 min. Homogenates (200 μl) were mixed with 800 μl ice cold immunoprecipitation buffer (1% NP-40, 1% Triton X-100, 1 mM $CaCl_2$ in TBS) and precleared with protein A-Sepharose (20 μl; Sigma Chem. Co.) or goat anti-rat IgG agarose (50 μl; Sigma Chem. Co.). The homogenates were incubated with rabbit anti-EcadEC5 (2.5 μl), DECMA-1 (1 μl), or ECCD-2 (2.5 μl) for 60 min, followed by protein A-Sepharose (20 μl), or goat anti-rat IgG agarose (50 μl) for an additional 30 min. The resin was collected by centrifugation, washed extensively with immunoprecipitation buffer, resuspended in SDS-PAGE sample buffer, and analyzed by SDS-PAGE and immunoblotting.

Immunohistochemistry

Sciatic nerves, obtained from 4% paraformaldehyde perfused mice and rats were cyroprotected with 20% sucrose and quick frozen in Tissue-Tek OCT compound (Miles Inc., Kankakee, IL) in liquid nitrogen. Cryosections (15 μm) were placed on TESPA (3-aminopropyltriethoxysilane; Sigma Chem. Co.) treated glass slides, stored at −80°C, and immunostained following standard procedures. To TESPA treat slides, slides were dipped in 2% TESPA (diluted in acetone) and then rinsed two times in acetone and one time in water. The slides were dried in a 50°C oven and stored at room temperature. For immunolabeling, sections were placed in 4% paraformaldehyde for 5 min, washed twice (10 min each) with TBS, and treated with blocking solution (5% normal goat serum, 0.1% Triton X-100 in TBS) for 15 min. The sections were then incubated with primary antibodies for 18 h at room temperature. For E-cadherin immunolabeling, affinity purified anti-EcadEC5 (25 μg/ml) was used; commericial antibodies were used according to the manufacturers' recommendations. After washing and blocking as described above, the sections were incubated with species specific fluorochrome-conjugated secondary antibodies (Jackson ImmunoResearch Laboratories, Inc.) for 30 min at room temperature and washed with TBS. Mounting medium (50 mM Tris, pH 8.6, 2.5% DABCO [1,4-diazabicyclo{2.2.2}octane; Sigma Chem. Co.], 90% glycerol) and cover slips were applied.

Because the mouse β-catenin antibodies were sensitive to paraformaldehyde fixation, methanol-fixed teased sciatic nerve fibers were used for double immunolabeling with mouse β-catenin and rabbit EcadEC5 antibodies. To obtain teased nerve fibers sciatic nerves were dissected from adult mice and placed in ice cold tissue culture medium (DME, 7.5% fetal bovine serum; GIBCO BRL, Gaithersburg, MD). After the epineurium was removed, the nerves were gently teased with a stainless steel probe to free individual fibers, fixed in −20°C methanol for 20 min and immunostained as described above.

After immunolabeling, sections and teased fibers were examined with a Leica TCS 4D confocal scanning microscope.

Confocal Microscopy Image Analysis

For each image, a data set from a series of incremental scans through the z axis of a tissue section was collected. Each scan produced a thin optical image of the x, y plane of the tissue section. Thus a complete data set could be used to generate three-dimensional reconstructions of labeled tissue, or a single scan could be used to show low-magnification images with exceptional clarity (see Fig. 4) and details of highly magnified morphological features (see Fig. 5 *B*, *insets*). However the z axis of single scans were often too thin to view structures in their entirety. Therefore geometric plane projections, which are "compressions" of three-dimensional data sets (i.e., a series of scans) into single flat images, were used to obtain images of nerve structure (see Figs. 5, *A* and *B*, and 7 *D*).

To generate views of labeled images from many different angles, the data from a series of scans was computationally rotated (see Fig. 5 *C*) and presented as geometric plan projections. Stereo images (see Fig. 6) were obtained by rotating geometric plane projections by 5°. Finally, video animation and three dimensional reconstructions, were used to aid in the interpretation of immunofluorescence patterns. All image processing was done using the Scanware software on the Leica TCS 4D confocal scanning microscope and Adobe Photoshop software.

Confocal images resulting from the analysis of tissue sections labeled with only one primary antibody are shown in glow color scale. This color scale shows the most intense labeling in white and the middle range intensities in yellow/orange. The use of the glow color scale seemed to yield superior visibility of the signal in the middle and low intensity ranges as compared to the gray color scale.

For double immunostained sections, data from two channels were collected simultaneously thus providing a precise colocalization, and individually analyzed to show the localization of each antigen. The data from one channel is indicated in green and data from the other channel is indicated in red. To examine the distribution of two antigens, data from both channels were overlayed to produce a single image in which regions of colocalization are indicated in yellow.

To compensate for the many scans required for three dimensional analyses low averaging values were used. This decreased the time required for each scan, and therefore allowed more scans to be performed before the signal quenched. However, one consequence of low averaging values was some statistical noise which produced a certain degree of graininess in the images (see Fig. 7, *C* and *D*).

Immunoelectron Microscopy

Sciatic nerves (8-d old) and intestine (18-d old) from Wistar rats were fixed by immersion in 4% paraforamldehyde, 0.1% glutaraldehyde, 0.5 mM $CaCl_2$, in 0.1 M sodium cacodylate buffer containing 3% sucrose, pH 7.4, for 2 h at room temperature. The tissue was rinsed in cacodylate buffer containing 3% sucrose, washed several times with phosphate buffer containing 3% sucrose, and stained with 0.25% tannic acid in the same buffer for 1 h at 4°C (subsequent steps were performed at 4°C). After several washes in phosphate sucrose buffer, aldehydes were quenched in 50 mM NH_4Cl in the same buffer. The tissue was then washed four times in 0.1 M maleate buffer, pH 6.2, containing 4% sucrose, followed by 2% uranyl acetate in maleate sucrose buffer for 1 h. The tissue was dehydrated to 90% ethanol (from 70% ethanol onward all steps were at −20°C), infiltrated with a 1:1 ratio of LR Gold (Electron Microscopy Sciences, Fort Washington, PA) and ethanol, followed by a 7:3 ratio of LR Gold and ethanol, and two changes of LR Gold for 2–3 h each. The tissue was infiltrated overnight in LR gold containing 0.5% benzoin methyl ether and embedded in gelatin capsules. Polymerization was by UV irradiation at a wavelength of 365 nm for 24 h at −20°C.

Sections on formvar-coated nickel grids were blocked with 1% BSA, 0.5% fish skin gelatin, 0.05% Triton X-100, 0.05% Tween 20 in Tris buffer (10 mM Tris, 500 mM NaCl, pH 7.4) for 30 min at room temperature, and incubated with affinity purified anti-EcadEC5(25 μg/ml) in the same buffer for 3 h at room temperature. Grids were washed four times with the above buffer and incubated for 1 h with goat anti-rabbit IgG conjugated to 10 nm gold (1:20; Amersham Corp., Arlington Heights, IL). The grids were then washed on drops of distilled water, fixed with 2.5% aqueous glutaraldehyde and rinsed in a stream of distilled water. After postfixing for 15 min with 2% aqueous OsO_4 the grids were stained with lead citrate and examined at 80 kV in a JEOL100CX electron microscope.

Results

E-Cadherin and Its Associated Proteins, α- and β-Catenin Are Expressed in Adult Peripheral Nerve

To generate specific polyclonal antibodies against E-cadherin, most of the EC5 domain (Fig. 1 *A*) of mouse E-cadherin (EcadEC5) was bacterially expressed as a GST fusion protein. The fifth extracellular domain was chosen because it is the least homologous region among the cadherins. For example, mouse N-cadherin, a likely candidate for expression in peripheral nerve, has only 34% identity in a 102-amino acid stretch with the EcadEC5 sequence and among the mammalian cadherin sequences in the Genbank database, bovine P-cadherin has the highest degree of identity (43% in a stretch of 85 amino acids). In both sequences the maximum

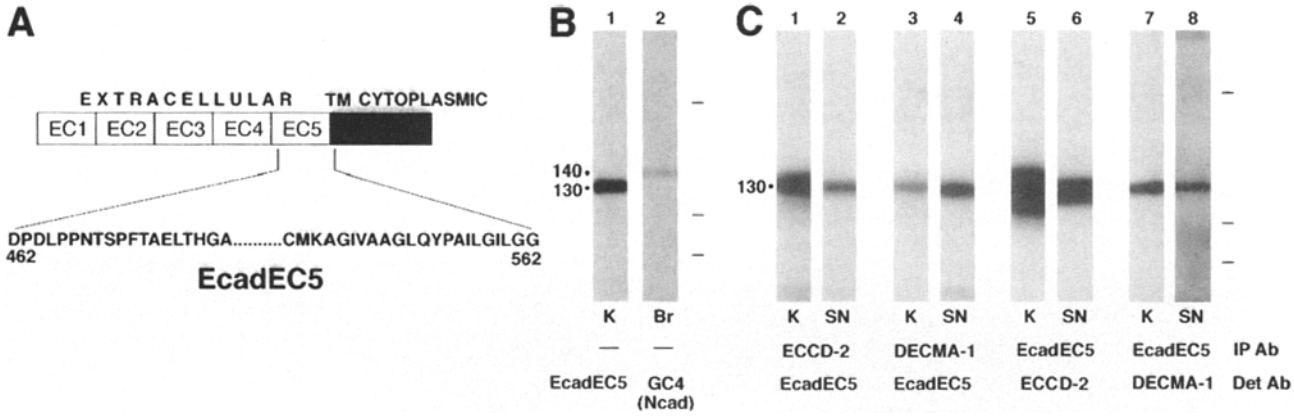

Figure 1. Characterization of EcadEC5 antibodies. (*A*) E-cadherin has a large extracellular domain (*white*) which can be divided into five homologous regions termed extracellular regions 1 through 5 (*EC1-EC5*), a short transmembrane domain (*black*) and a cytoplasmic domain (*gray*). EC5 is the least homologous region and was used to generate specific polyclonal antibodies. The antigenic epitope for EcadEC5 consists of 82 amino acids from EC5 and 19 amino acids from the transmembrane domain. (*B*) Kidney (*K*) and brain homogenates (*Br*) were separated by SDS-PAGE and transferred to nitrocellulose. E-Cadherin was detected in kidney homogenates with anti-EcadEC5 (lane *1*) and N-cadherin was detected in brain homogenates with CG-4 (anti-ACAM, lane *2*). Molecular weight standards (200, 116, and 97 kD) are indicated to the right of the blot. (*C*) E-cadherin was immunoprecipitated from mouse kidney (*K*, lanes *1*, *3*, *5*, and *7*) and sciatic nerve (*SN*, lanes *2*, *4*, *6*, and *8*) homogenates using ECCD-2 (lanes *1* and *2*), DECMA-1 (lanes *3* and *4*) or anti-EcadEC5 (lanes *5–8*), separated by SDS-PAGE, and transferred to nitrocellulose. Immunoprecipitated protein was detected using anti-EcadEC5 (lanes *1–4*), ECCD-2 (lanes *5* and *6*) or DECMA-1 (lanes *7* and *8*). (*IP Ab*) Immunoprecipitation antibody; (*Det Ab*) detection antibody. Molecular weight standards (200, 116, and 97 kD) are indicated to the right of the blot.

number of contiguous identical amino acids is four. Thus, we considered it unlikely that antibodies directed against the EcadEC5 epitope would recognize either P- or N-cadherin.

On immunoblots of kidney homogenates, a well-characterized source of E-cadherin (Gumbiner and Simons, 1987; Behrens et al., 1989), anti-EcadEC5 detected a single band of 130 kD (Fig. 1 *B*, lane *1*). This relative molecular mass was slightly larger than that reported for E-cadherin in other cells (120 kD, Nagafuchi et al., 1987), and was similar to the reported relative molecular mass of N-cadherin (130 kD). To confirm that anti-EcadEC5 detected E-cadherin and not N-cadherin, anti-ACAM (clone GC-4), a commercially available N-cadherin antibody, was used to detect N-cadherin in brain homogenates. Anti-ACAM detected a single band of 140 kD in brain homogenates (Fig. 1 *B*, lane 2), which migrated more slowly than E-cadherin (Fig. 1 *B*, lane *1*), strongly indicating that anti-EcadEC5 does not recognize N-cadherin.

To verify the specificity of anti-EcadEC5, E-cadherin was immunoprecipitated from adult kidney and sciatic nerve homogenates with ECCD-2 or DECMA-1 and detected by immunoblotting with anti-EcadEC5 (Fig. 1 *C*, lanes *1–4*). The reverse experiment, in which E-cadherin was immunoprecipitated with anti-EcadEC5 and detected with ECCD-2 or DECMA-1, was also performed (Fig. 1 *C*, lanes *5–8*). DECMA-1 is a monoclonal antibody which blocks E-cadherin function and recognizes an epitope in the EC5 region of E-cadherin (Ozawa et al., 1989). ECCD-2 is a monoclonal antibody which recognizes E-cadherin but does not inhibit its function (Shirayosi et al., 1986). In all immunoprecipitation experiments, single bands, having identical molecular masses of 130 kD, were detected in the kidney (Fig. 1 *C*, lanes *1*, *3*, *5*, and *7*) and sciatic nerve (Fig. 1 *C*, lanes *2*, *4*, *6* and *8*) homogenates. Note that when anti-EcadEC5 was used to immunoprecipitate E-cadherin from kidney homogenates, a very intense broad signal was obtained upon detection with ECCD-2 (Fig. 1 *C*, lane *5*). This was likely due to the efficiency of EcadEC5, a polyclonal antibody, as an immunoprecipitating agent, and the high reactivity of ECCD-2 with E-cadherin. The results of the immunoprecipitation experiments demonstrate that anti-EcadEC5 specifically recognizes the same protein as ECCD-2 and DECMA-1, i.e., E-cadherin.

In sciatic nerve homogenates, ECCD-2 (Fig. 2 *A*, lane *1*) and anti-EcadEC5 (Fig. 2 *A*, lane *2*) both detect bands of ~130 kD. This band was not detectable in competition experiments in which anti-EcadEC5 and the fusion protein GST-EcadEC5 were preincubated (Fig. 2 *A*, lane *3*). In epithelial cells, E-cadherin associates with α-, β-, and γ-catenin, a family of cytoplasmic proteins whose interactions with cadherins appear to be required for adhesion (Hirano et al., 1992; Kintner, 1992). Therefore we probed identical immunoblots with α- and β-catenin antibodies and found that bands having molecular masses of ~108 and ~95 kD, which corresponded to the relative molecular masses of α- and β-catenins, respectively (Ozawa et al., 1989; Hinck et al., 1994) were detected in sciatic nerve homogenates (Fig. 2 *A*, lanes *4* and *5*). E-cadherin and α- and β-catenin were also found in osmotically shocked membrane fractions of sciatic and trigeminal nerves (Fig. 2 *B*). Because this membrane fraction is known to consist almost entirely of Schwann cell plasma membranes and myelin, E-cadherin in this fraction was likely to be derived from Schwann cells. The presence of α- and β-catenins in these membranes suggested that they were associated with E-cadherin, and/or perhaps other as yet unidentified cadherins.

EcadEC5 Antibodies Specifically Recognize Adherens Junctions

Previous immuno-electron microscopy studies have established that E-cadherin is a marker of adherens junctions in

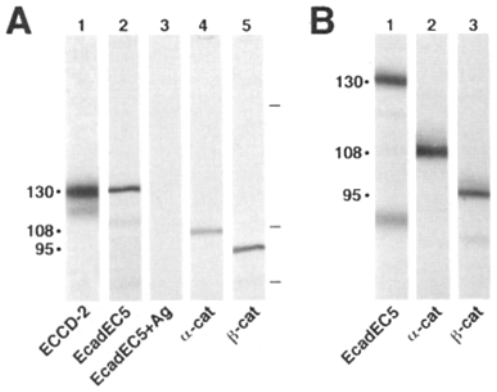

Figure 2. E-cadherin and α- and β-catenins are expressed in peripheral nerve. Adult mouse sciatic nerve homogenates (*A*) and an osmotically shocked membrane fraction from trigeminal nerves (*B*) were separated by SDS-PAGE, transferred to nitrocellulose and immunostained using ECCD-2 (*A*, lane *1*), affinity purified anti-EcadEC5 (*A*, lanes *2* and *3*, *B*, lane *1*), anti-α-catenin (*A*, lane *4*, *B* lane *2*) or anti-β-catenin (*A*, lane *5*, *B*, lane *3*). Ag, GST-EcadEC5. Molecular weight standards (200, 116 and 97 kD) are indicated to the right of the blot in *A*.

rat intestine (Boller et al., 1985). To verify the specificity of EcadEC5 antibodies that we raised for the localization studies, anti-EcadEC5 was tested on thin sections of rat intestinal tissue (Fig. 3). At the lateral boundaries of longitudinally (Fig. 3 *A*) and obliquely (Fig. 3 *B*) sectioned rat intestine, adherens junctions (*arrows*) and desmosomes (*A*, *arrowheads* and *B*, *asterisk*) are evident. EcadEC5 antibodies strongly and specifically labeled adherens junctions (Fig. 3, *arrows*) but did not label desmosomes (*arrowheads*) or any other structures.

E-Cadherin Has a Restricted Distribution within the Cytoplasmic Compartments of Peripheral Nerve Schwann Cells, and is Highly Concentrated in Schmidt-Lanterman Incisures and Paranodes

In tissue sections anti-EcadEC5 intensely labeled trigeminal and sciatic nerves from mice and rats. Confocal microscopy was routinely used to localize E-cadherin distribution in these tissues. In cross sections of E-cadherin immunolabeled peripheral nerve, individual fibers were easily identified by circumferential fluorescence (Fig. 4 *A*), indicating that E-cadherin was present in the outer cytoplasmic loops of Schwann cells. At the outer loop, at least one intense fluorescent spot could be detected (Fig. 4 *A*, *small arrows*), indicat-

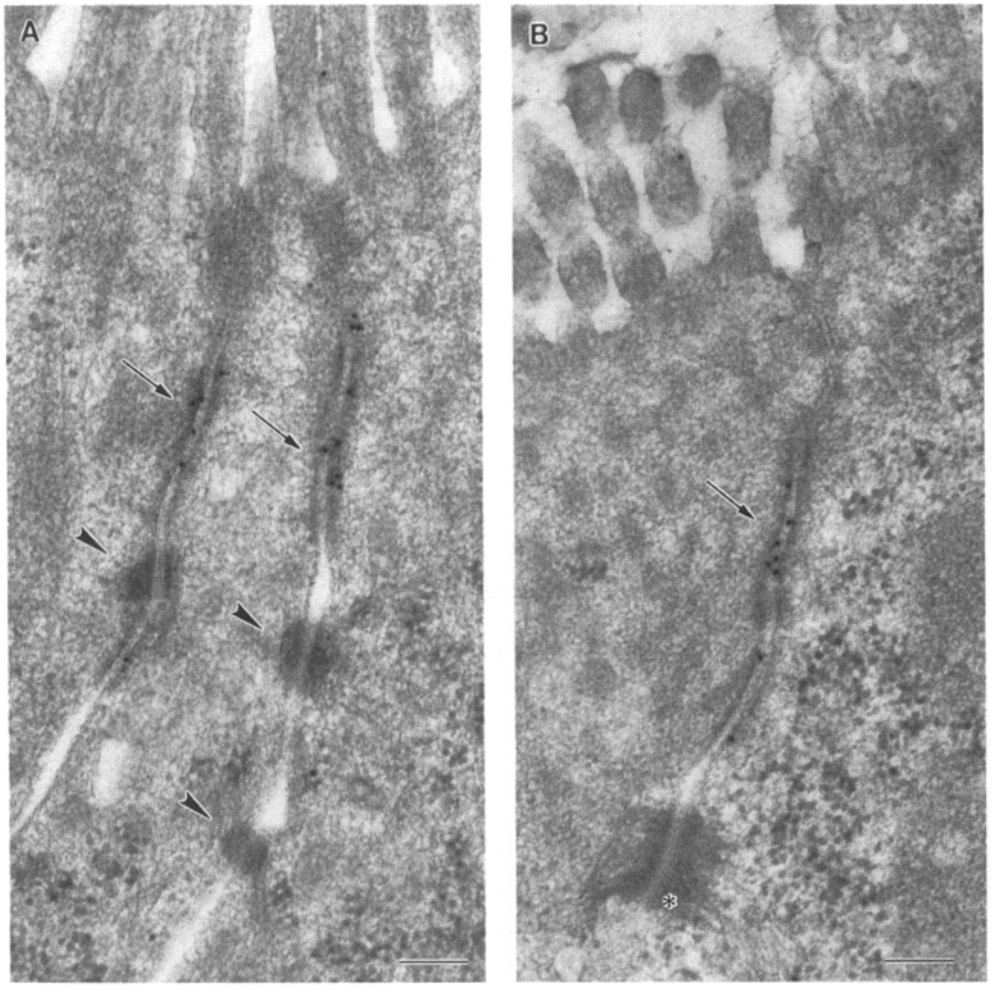

Figure 3. EcadEC5 antibodies specifically recognize adherens junctions. Longitudinally (*A*) and obliquely (*B*) sectioned rat intestinal tissue was labeled with EcadEC5 antibodies. The apically located microvilli are at the top of the figure. At the lateral surface, adherens junctions are strongly labeled with EcadEC5 antibodies (*arrows*). Desmosomes (*A*, *arrowheads*), including those with an extensive filamentous network (*B*, *asterisk*), are devoid of label. Bars, 0.1 μm.

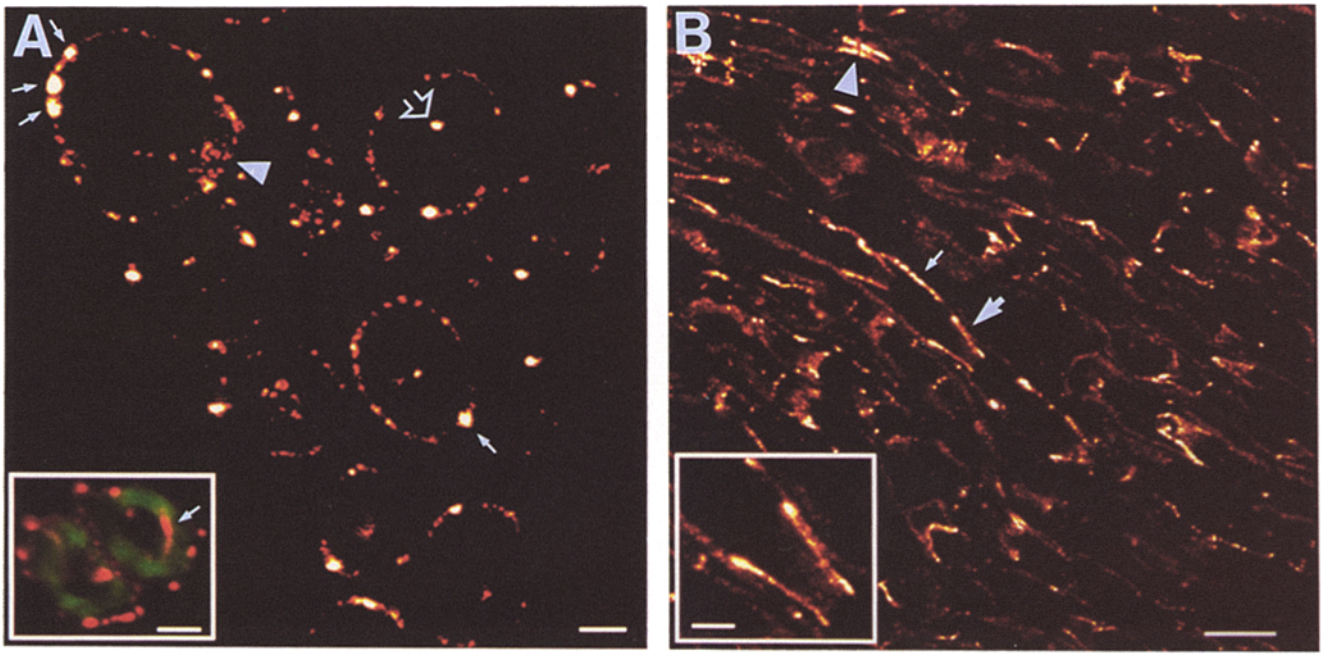

Figure 4. E-cadherin localizes to the cytoplasmic compartments of Schwann cells. Cryosections of adult mouse sciatic nerve were immunolabeled with anti-EcadEC5 and viewed by confocal microscopy. (*A*) In cross section, anti-EcadEC5 localized to numerous puncta in the outer loops (*small arrows*) and a single dot in the inner loops (*open arrow*). Labeling of the Schwann cell cytoplasm (*arrowhead*) was faint. The inset in *A* shows two nerve fibers labeled with EcadEC5 (*red*) and diD (*green*), a lipophilic dye that intensely labels myelin. A cross section of a Schmidt-Lanterman incisure, labeled by anti-EcadEC5, is apparent in this field (*A*, *inset*, *arrow*). (*B*) In longitudinal section, anti-EcadEC5 labeling revealed the classic morphology of Schmidt-Lanterman incisures (large arrow, and see *inset*). Anti-EcadEC5 also labeled the outer loop of nerve fibers (*small arrow*) and the paranodes (*arrowhead*). (See Fig. 5 *A* for the intensity scale.) Bars: (*A* and *B*) 10 μm; (*insets*) 2 μm.

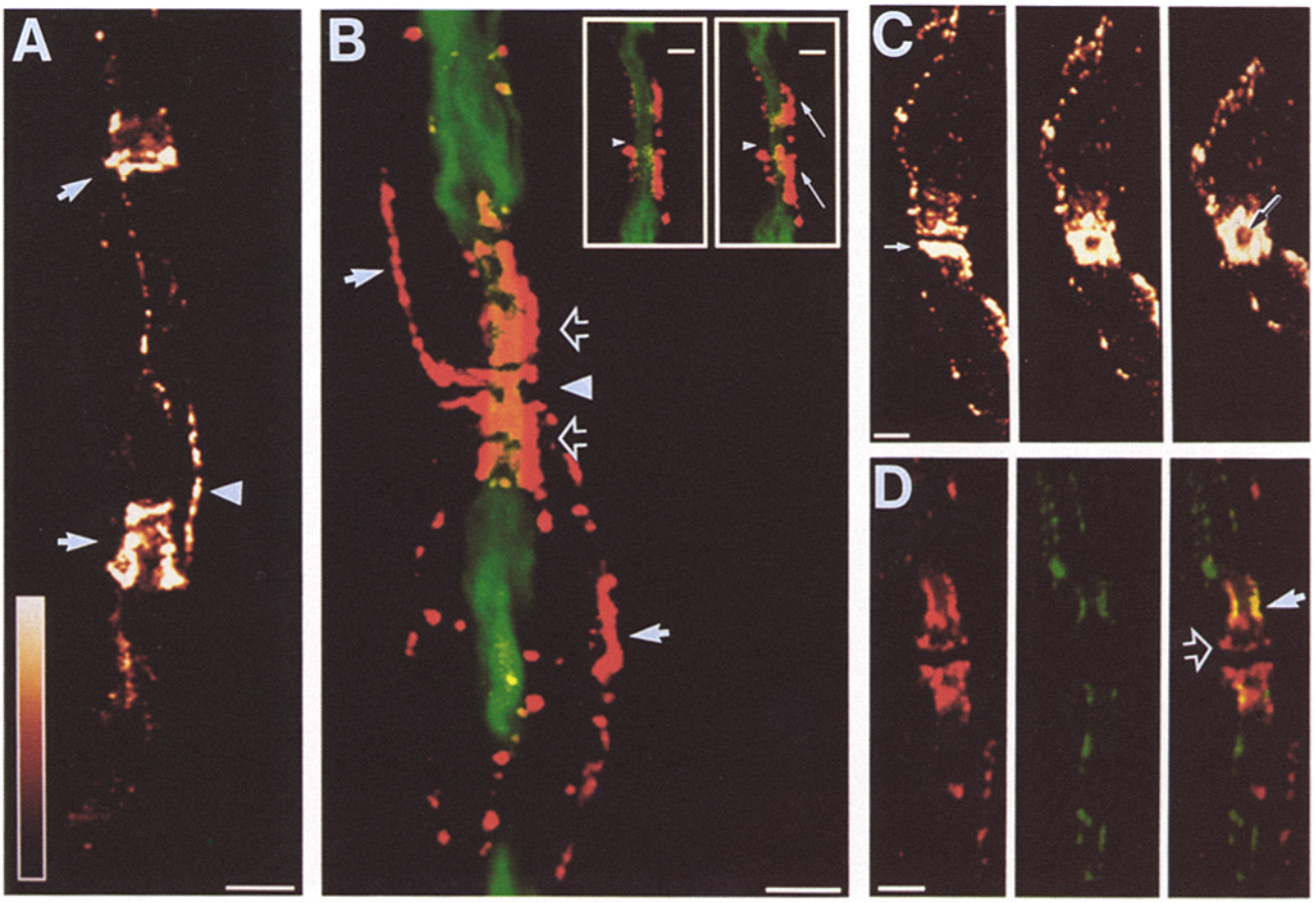

ing that E-cadherin was concentrated in discrete subdomains. Punctate labeling at the inner loop was occasionally noted (Fig. 4 *A*, *open arrow*), but, in contrast to the outer loop, only one E-cadherin site per inner loop was detected. The Schwann cell cytoplasm was also faintly labeled (Fig. 4 *A*, *arrowhead*), consistent with synthesis of this transmembrane protein on rough endoplasmic reticulum and post-translational processing in the Golgi apparatus. Significantly, compact myelin and axons were devoid of E-cadherin immunofluoresence. Fig. 4 *A* (*inset*) shows two myelinated axons labeled with E-cadherin (red) and diD (green), a lipophilic dye which intensely labels myelin. Note the absence of E-cadherin in the myelin and axons, and the punctate E-cadherin labeling surrounding the myelin, which corresponds to the outer loop. The arrow (Fig. 4 *A*, *inset*) indicates a cross section of a Schmidt-Lanterman incisure, which was also intensely labeled by anti-EcadEC5. In longitudinal section, the outer loops were labeled in discontinuous tracts resembling "beads on a string" that were parallel to the axes of the fibers (Fig. 4 *B*, *small arrow*). It is interesting to note that, in contrast to the outer loop, clearly delineated E-cadherin tracts were not found at the inner loops in longitudinal sections. Longitudinal sectioning also revealed that E-cadherin was highly concentrated in Schmidt-Lanterman incisures (Fig. 4 *B*, *large arrow* and *inset*) and paranodes (Fig. 4 *B*, *arrowhead*). Thus in Schwann cells, E-cadherin is found exclusively in the outer and inner loops, paranodes, Schmidt-Lanterman incisures, i.e. in the regions which comprise the continuous cytoplasmic channel network that forms the boundary domain of compact myelin.

At high resolution, E-cadherin immunofluorescence clearly yielded the classical funnel-shaped image of Schmidt-Lanterman incisures (Hall and Williams, 1970; Ghabriel and Allt, 1981) in both trigeminal and sciatic nerves (Fig. 5 *A*, *arrows*). These thin spiral channels interrupt compact myelin within the internode and have been implicated in the metabolic maintenance of the myelin sheath (Ghabriel and Allt, 1981). At both ends of an incisure ring-like structures which completely encircled the axon were detected (Fig. 5 *A*), with slightly more intense labeling at the periphery (see also Fig. 4 *B*, *inset*). Often Schmidt-Lanterman incisures were linked to each other by E-cadherin-positive tracts (Fig. 5 *A*, *arrowhead*).

Most interestingly, anti-EcadEC5 strongly highlighted the paranodal region (Fig. 5, *B–D*). To obtain a highly detailed image of E-cadherin localization, a series of 44 confocal scans through a "paranode-node-paranode" was analyzed using three dimensional reconstructions and video animation, and presented as a geometric plane projection (Fig. 5 *B*). E-Cadherin labeling is indicated in red and the axon, demarcated by anti-neurofilament labeling, is shown in green. The node of Ranvier is indicated by the arrowhead. The high degree of color saturation in the EcadEC5 channel results from an intense immunofluorescent signal and photodetector settings optimized for low signal levels. These conditions were used to ensure detection of all E-cadherin positive structures. E-Cadherin immunofluorescence flanked the narrowed paranodal axon, precisely terminating at the locus where the axonal diameter enlarged (Fig. 5 *B*, *open arrows*). Enlargements of single scans of the nodal region showed that E-cadherin was absent from the node of Ranvier (Fig. 5 *B*, *insets*, *arrowheads*). One feature of E-cadherin localization, which was revealed by three-dimensional imaging, was that E-cadherin helically encircled the narrowed paranodal axon. This helicity is suggested in single optical images (Fig. 5 *B*, *right inset*, *arrows*), and is depicted on the cover of this issue. E-cadherin immunolabeling of the outer loop is also apparent (Fig. 5 *B*, *white arrows*).

Another interesting feature of paranodal E-cadherin distribution was that at the limiting edge of some, but not all, paranodes, E-cadherin completely encircled the axon forming a cylindrical collar. Fig. 5 *C* is a series of rotations around the x axis of an anti-EcadEC5 immunolabeled paranodal region. The left panel (0°) shows the paranodal region in longitudinal section; the right panel (50°) shows the paranodal region in a slightly oblique cross section. As the

---

Figure 5. E-cadherin is highly concentrated in Schmidt-Lanterman incisures and paranodes in sciatic nerve. (*A*) Confocal image of two Schmidt-Lanterman incisures (*arrows*) labeled with anti-EcadEC5. A thin E-cadherin positive tract (*arrowhead*) appears to connect the incisures. To reconstruct the incisures, two 0.27-μm incremental scans in the z axis were merged into a single image. The scale at the right indicates the glow scale labeling intensity. (*B*) Confocal image of a paranodal region immunolabeled with anti-EcadEC5 (*red*) and anti-neurofilament (*green*). A geometric plane projection of the paranode was created by merging 44 0.1-μm incremental scans in the z axis into a single image. The color saturation in the anti-EcadEC5 channel (*red*) was the result of an intense signal and photodetector settings optimized for low signal levels. These conditions were used to ensure detection of all E-cadherin-positive structures. Signals from each antibody were simultaneously collected as two separate data sets, and overlaid to produce a single image. Neurofilament immunolabeling demarcates the axon. Anti-EcadEC5 labeled paranodal regions (*open arrows*), and outer loops (*white arrows*) but did not label the node of Ranvier (*arrowhead*). Note that yellow does not indicate regions of colocalization (see text). The left inset is an individual scan (z axis, 0.1 μm) taken at the midpoint of the axon and shows that anti-EcadEC5 labeling is situated at the edge of the axon, not in the axon. The right inset is an individual scan (z axis, 0.1 μm) taken in the top quarter of the nerve fiber and indicates that the adaxonal labeling (*arrows*) is helically orientated around the axon. In both insets, the node of Ranvier is indicated by the arrowhead. (*C*) Rotations around the x axis of an EcadEC5-labeled paranode. 29 scans of a longitudinally sectioned paranode, taken at 0.13-μm increments in the z axis, were merged into a single image to create a geometric plane projection of the paranodal region (0° *left*). The geometric plane projection was computationally rotated around the x axis by 30° (*middle*) and by 50° (*right*). The disc indicated by the arrow (*left*) represents anti-EcadEC5 paranodal labeling which completely encircles the axon and forms a paranodal collar. The paranodal collar is clearly evident after rotating the image around the x axis (*middle* and *right*). In the right panel, the axon, which is devoid of E-cadherin labeling, is indicated by the arrow. (See *A* for intensity scale.) (*D*) confocal images of a paranode labeled with rabbit anti-EcadC5 (*left*, *red*) and mouse anti-MAG (*middle*, *green*). The overlay (*right*) shows regions of E-cadherin and MAG colocalization (*yellow*). Two confocal scans of a longitudinally sectioned paranodal region, taken at 0.11-μm increments in the z axis, were merged into a geometric plane projection. The overlay (*right*) indicates that both anti-EcadEC5 (*red*) and anti-MAG (*green*) demonstrate adaxonal labeling (*open arrow*, *yellow*), but only anti-EcadEC5 labels the paranodal collar (*solid arrow*). Bars: (*A*) 5 μm; (*B*) 2 μm; (*insets*, 1 μm; (*C* and *D*) 2 μm.

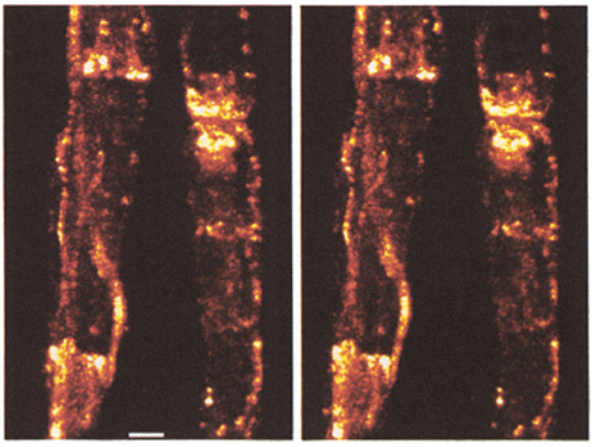

Figure 6. Stereo image of E-cadherin positive tracts in two sciatic nerve fibers. Confocal scans were merged into geometric plane projections which were then computationally rotated around the y axis. The two images, differing by 5°, can be paired to produce a stereo image. Bar, 2 μm.

fiber was rotated, the flattened disc in the left panel (Fig. 5 *C*, *arrow*), became a hollow E-cadherin positive ring encircling the axon (Fig. 5 *C*, *right*, *arrow*; see also Fig. 6, *right fiber*). In most paranodes where collars were found, two collars, one at the limiting edge of each internode were observed.

In Schwann cells, E-cadherin distribution was remarkably similar but not identical, to that of an IgCAM superfamily protein, MAG (myelin-associated glycoprotein). While both proteins were restricted to the cytoplasmic channels of Schwann cells, they did not exhibit an exact colocalization. For example, in the inner loop, MAG was evenly distributed (Trapp et al., 1989) while E-cadherin was restricted to a single punctate site (see Fig. 4 *A*). In addition, in the paranodal region, both E-cadherin and MAG flanked the paranodal axon (Fig. 5 *D*, *solid arrow*, *yellow*), but E-cadherin, alone, formed a paranodal collar (Fig. 5 *D*, *open arrow*, *red*).

Helical E-cadherin Tracts Are in Register Across Adjacent Internodes

A distinguishing feature of E-cadherin distribution in the internode was its organization into discontinuous longitudinal tracts that wound helically along the periphery of the Schwann cell in the outer loops (Fig. 6). Indeed, the punctate fluorescence in the outer loop observed in cross sections (see Fig. 4 *A*) corresponded to labeling of the tracts. As the E-cadherin tracts wove among the outer loop, they crisscrossed and often extended from one Schmidt-Lanterman incisure to the next (see also Fig. 5 *A*), indicating that E-cadherin was part of a highly organized substructure within the entire cytoplasmic channel network of Schwann cells. Video animation revealed that the helical paths delineated by E-cadherin continued in register from internode to

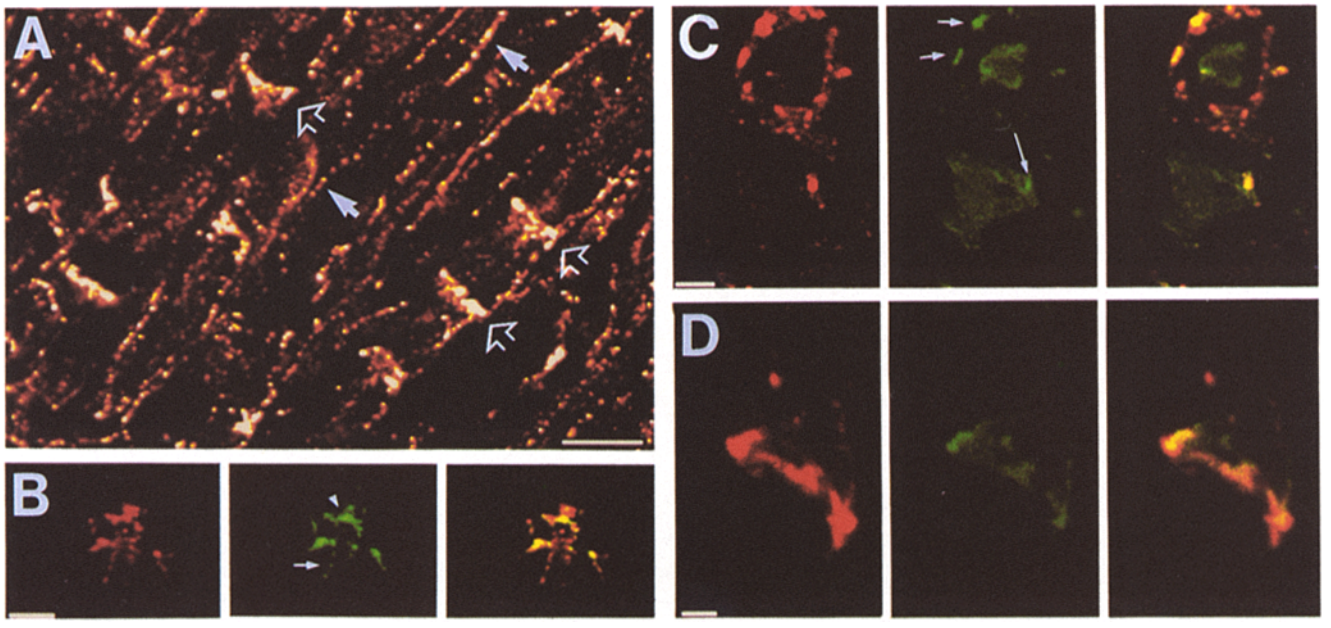

Figure 7. β-catenin and F-actin colocalize in peripheral nerve fibers. (*A*) Peripheral nerve, immunolabeled with anti-β-catenin was analyzed by confocal microscopy. Two scans, taken at 1.7-μm increments in the z axis, were merged into a geometric plane projection. The open arrows demarcate labeling of Schmidt-Lanterman incisures and the solid arrows indicate labeling of the outer loops. (*B*) Confocal image of a paranodal region immunolabeled with anti-EcadEC5 (*left*, *red*) and anti-β-catenin (*middle*, *green*). The regions of colocalization are indicated in yellow in the overlay (*right*). A single confocal scan was taken through the midpoint of an obliquely cut paranode. Both adaxonal labeling (*arrow*) and paranodal collar labeling (*arrowhead*) were apparent with anti-β-catenin (*middle*). The overlay (*right*) shows colocalization of E-cadherin and β-catenin (*yellow*). (*C*) Confocal image of two nerve fibers immunolabeled with anti-EcadEC5 (*left*) and phalloidin (*middle*) which binds to F-actin. Two scans, taken at 1.3-μm increments in the z axis, were merged into a geometric plane projection. The graininess in this set of images is due to low averaging values used during data collection. F-Actin (*middle*) is found in the outer loop (*short arrows*) and inner loop (*long arrow*). These regions colocalize with anti-EcadEC5 (*right*, *yellow*). (*D*) Confocal image of a Schmidt-Lanterman incisure immunolabeled with E-cadherin (*left*) and phalloidin (*middle*). Nine confocal scans, taken at 0.54-μm increments in the z axis, were merged into a geometric plane projection. The overlay (*right*) shows E-cadherin and F-actin colocalization (*yellow*) in Schmidt-Lanterman incisures. Bars: (*A*) 10 μm; (*B* and *C*) 2 μm; (*D*) 1 μm.

internode. This novel observation suggested, surprisingly, that adjacent Schwann cells may be functionally associated with one another. Thus the morphology of the E-cadherin network revealed a previously unsuspected organization of Schwann cells into what might be a globally interactive unit.

β-Catenin and F-Actin Colocalize with E-Cadherin in the Outer and Inner Loops and at Schmidt-Lanterman Incisures and Paranodes

Low magnification confocal images of β-catenin immunolabeled peripheral nerve were similar to those observed for E-cadherin labeled tissue (Fig. 7 *A*). Schmidt-Lanterman incisures (Fig. 7 *A*, *open arrows*) and labeling at the outer loop (Fig. 7 *A*, *white arrows*) were clearly visible. At the paranodes, β-catenin flanked the axon (Fig. 7 *B*, *middle*) and formed a paranodal collar (Fig. 7 *B*, *arrowhead*), thus demonstrating a precise colocalization with E-cadherin (Fig. 7 *B*, *right*, *yellow*).

F-Actin, another protein which associates with E-cadherin, also localizes to E-cadherin positive regions (Fig. 7, *C* and *D*). F-actin, labeled by phalloidin, had a punctate appearance in the outer loop (Fig. 7 *C*, *middle*, *short arrows*) which precisely colocalized with E-cadherin (Fig. 7 *C*, *right*). In the inner loop, a single distinct spot of F-actin was found (Fig. 7 *C*, *long arrow*), which co-distributed with E-cadherin (Fig. 7 *C*, *right*, *yellow*). Finally F-actin (Fig. 7 *D*, *middle*) and E-cadherin (Fig. 7 *D*, *left*) colocalized in Schmidt-Lanterman incisures (Fig. 7 *D*, *right*, *yellow*). The graininess in Fig. 7 (*C* and *D*) is from statistical noise produced when using low averaging values during data collection, and is not due to a weak signal. Sciatic and trigeminal nerves were also examined for the presence of vinculin, another protein which is associated with E-cadherin adhesion complexes (Geiger and Ginsberg, 1991). Preliminary data indicated that vinculin antibodies strongly labeled blood vessels in peripheral nerve but did not colocalize with E-cadherin (data not shown). The co-distributions of E-cadherin with β-catenin and F-actin provide strong evidence that these proteins may organize into an adhesion complex that has characteristics of adherens junctions and is integral to the stability of the inner and outer loops, Schmidt-Lanterman incisures and the paranodes.

E-Cadherin Mediates Adhesion within an Individual Schwann Cell

A striking finding was that by immunoelectron microscopy, E-cadherin strongly labeled Schwann cell membranes associated with cytoplasmic densities in the paranodes (Fig. 8), Schmidt-Lanterman incisures (Fig. 9) and outer mesaxons (Fig. 10, *B–D*). No E-cadherin was observed at the Schwann

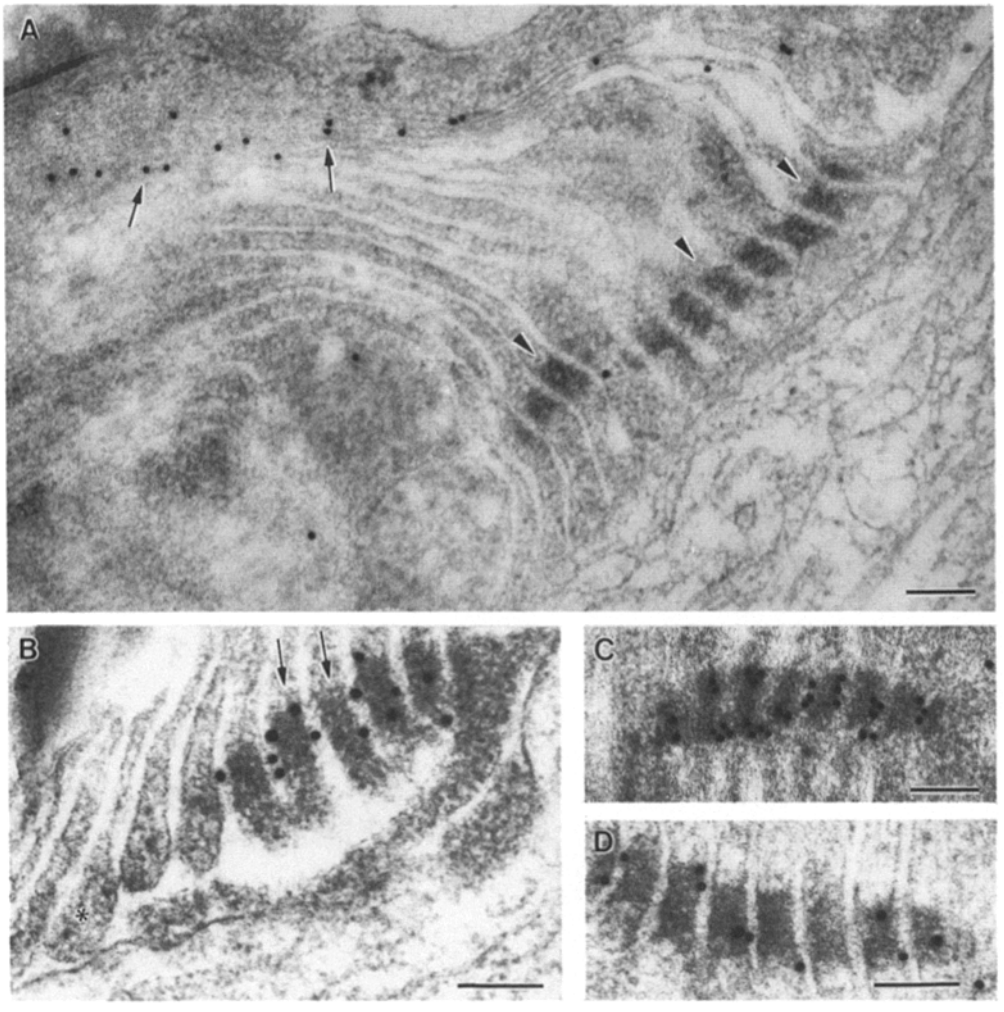

Figure 8. E-cadherin localizes to densities in the paranodal channels. Immunoelectron microscopy of sciatic nerve from 7-d-old mice and rats labeled with anti-P_0 (*A*) or anti-EcadEC5 (*B–D*). Anti-EcadEC5 intensely labels densities in the paranode (*B*, *arrows*). Note the extensive labeling of the densities in *C*. In *D*, the narrowing of the cytoplasm and the widening of the intracellular space is apparent. In a control P_0-labeled paranode (*A*) myelin (*arrows*) is labeled, but the densities (*arrowheads*) remain unlabeled. Bars, 0.1 μm.

cell–axonal interface, nor between the membranes of two Schwann cells. Thus, in the PNS, E-cadherin is unusual in that it mediates adhesion between membranes elaborated by an individual cell.

In longitudinally sectioned paranodes, cytoplasmic densities were strongly labeled with anti–EcadEC5 (Figs. 8, *B–D*). In control sections, P_0, the major glycoprotein of peripheral nerve myelin localized specifically to compact myelin (Fig. 8 *A*, *arrows*), and was absent from the densities (Fig. 8 *A*, *arrowheads*). Loops extending from the innermost myelin lamellae consistently contained the most well developed densities (Fig. 8 *B*, *arrows*), while the outermost turns (Fig. 8 *B*, *asterisk*) were often devoid of densities and E-cadherin labeling. Since the tissue used for the immunoelectron microscopy was obtained from 7-d-old animals, the preferential labeling of the inner turns may have been related to a developmentally transient event. We did not observe immunogold labeling of structures which would correspond to the collars seen in some paranodes by light microscopy (see Figs. 5 *C* and 7). The absence of such labeling may be developmentally related and/or it could be due to the lower sensitivity of immunoelectron microscopy. The arrangement of the plaques across several turns of the paranodal channel produced a large zonula-like junctional complex. Within the junctional array, there was a distinct narrowing of the cytoplasm from 85 to 45 nm (Fig. 8 *D*), accompanied by a local widening of the extracellular space (see also Harkin, 1964). In addition the densities extended across the full length of the cytoplasm, in effect dividing the paranodal channel into two separate compartments.

E-Cadherin is also highly concentrated in densities found in Schmidt-Lanterman incisures. Fig. 9 *A* is a transverse section of a developing myelin sheath showing what is likely to be a forming Schmidt-Lanterman incisure. At the periphery of the sheath, three densities are specifically labeled by anti–EcadEC5 (Fig. 9 *A*, *arrows*). Two well-developed Schmidt-Lanterman incisures and their associated densities (Fig. 9 *B*, *arrows*) are shown in a P_0-labeled control section. As in the paranodal channel, densities in the Schmidt-Lanterman incisures are highly ordered and aligned in contiguous cytoplasmic wraps. E-Cadherin thus may have an important role in the formation of Schmidt-Lanterman incisures.

At the outer loop, E-cadherin was associated with densities that were either macular (Fig. 10 *D*, *arrows*) or reasonably extensive (≥350 nm, Fig. 10 *C*). E-cadherin was also present at densities at the outer mesaxon (Fig. 10 *B*). The presence of these profiles directly correlated with the punctate and linear E-cadherin fluorescence patterns we detected along outer loops by confocal microscopy (see Figs. 4, 5 *A*, and 6). The inner mesaxon was the only region that consistently showed E-cadherin localization in the absence of cytoplasmic densities (Fig. 10 *A*, *arrows*). However, densities at some inner mesaxons were noted by Bunge et al. (1989) in sheaths that had only a few compact wraps. The labeled inner mesaxons that we observed were in sheaths with numerous turns of compact myelin. At the inner mesaxon, it is possible that the appearance of these densities may be transiently coordinated with the state of myelin bilayer compaction. The presence of E-cadherin together with the absence of densities suggests that only relatively weak adhesion could be required at the inner mesaxon after compaction has occurred. In contrast, the presence of dense plaques in the paranodes and outer mesaxons is indicative of strong adhesive and mechanical stabilization in these regions.

Discussion

The data presented here reveal E-cadherin to be an important component in the cytoarchitecture of individual Schwann cells. In other cell types, cadherins mediate intercellular adhesion. Even in peripheral nerve, it has been shown that

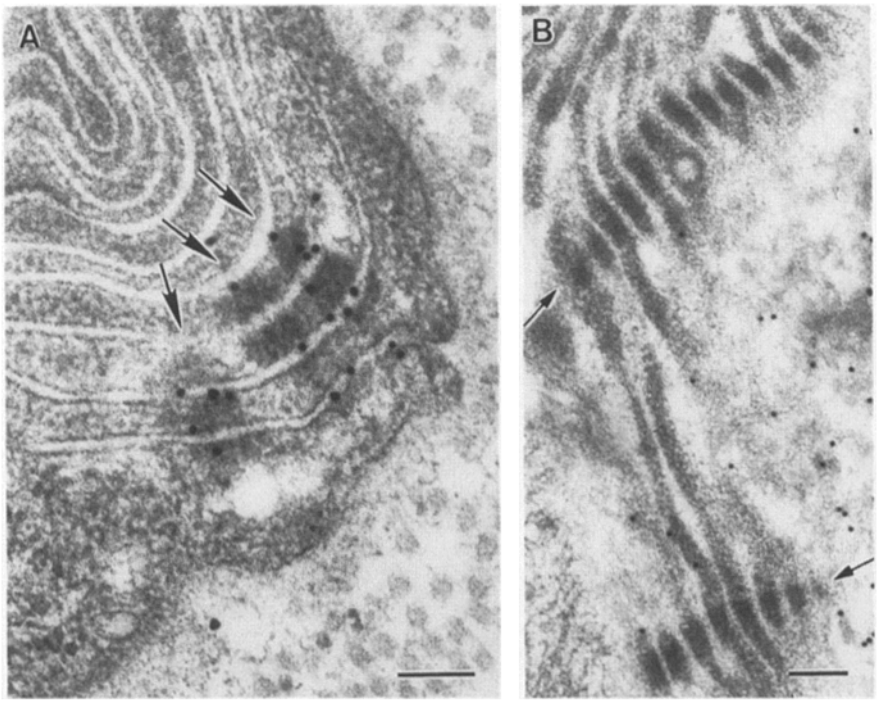

Figure 9. Distribution of cytoplasmic plaques in Schmidt-Lanterman incisures. Immunoelectron microscopy of Schmidt-Lanterman incisures labeled with anti–EcadEC5. In *A*, the arrows indicate three labeled densities in a forming Schmidt-Lanterman incisure. In a control P_0-labeled incisure (*B*), labeling of myelin is apparent, but the densities (*arrows*) remain unlabeled. Bars, 0.1 μm.

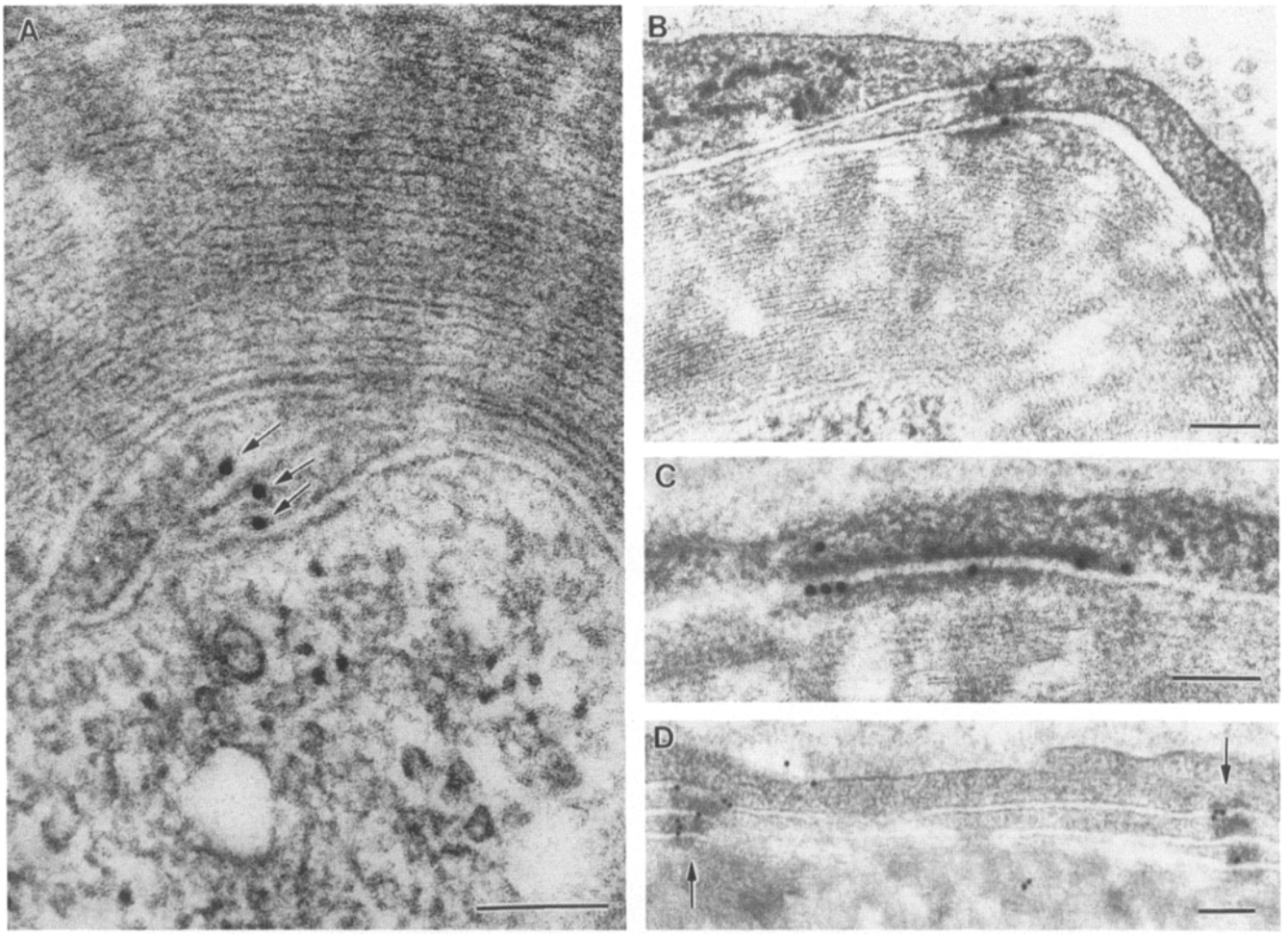

Figure 10. Distribution of E-cadherin in the inner and outer mesaxons and the outer loops of Schwann cells. Immunoelectron microscopy of Schwann cells labeled with anti-EcadEC5. (*A*) E-cadherin is present at the inner mesaxon (*arrows*) in the absence of a well-developed plaque. Conversely, at the outer mesaxon, E-cadherin is associated with well-developed densities (*B*). In the outer loop, anti-EcadEC5 localizes to large, extensive densities (*C*) and to macular densities (*D, arrows*). Bars, 0.1 μm.

satellite cells, which surround dorsal root ganglion cells, express E-cadherin at cell to cell contact sites (Shimamura et al., 1992; Uchiyama et al., 1994). However, in the Schwann cell, E-cadherin is unique in that it mediates adhesion between membranes elaborated by a single cell. E-cadherin was not detected between two Schwann cells nor between Schwann cells and the axon. In Schwann cells, E-cadherin localizes to densities which we have designated as autotypic adherens-type junctions, in contrast to homotypic (between two similar cell types) and heterotypic (between two different cell types) junctions. To our knowledge this is the first documentation of functional E-cadherin mediated adhesion within an individual cell.

Densities in the paranodes (Harkin, 1964), mesaxons (Bunge et al., 1989) and Schmidt-Lanterman incisures (Hall and Williams, 1970) have been noted but infrequently discussed. It is now clear that these densities are components of an adherens junctional system that serves to anchor adjacent membranes. The argument that these are adherens-type junctions is based on their ultrastructural morphology as well as the presence of E-cadherin, and likely β-catenin and F-actin, hallmark molecules of adherens junctions found in other tissues (Boller et al., 1985; Volk and Geiger, 1986*a*, *b*; Le Bivic et al., 1990; Geiger and Ginsberg, 1991; Geiger and Ayalon, 1992). Despite the similarities with classical junctions, Schwann cell adherens junctions are unusual in that the subplasmalemmal plaque traverses the cytoplasmic compartment and appears to fuse with the adjacent plaque.

E-Cadherin adhesion loci in the Schwann cell are distributed throughout the cytoplasmic channel network, which is most easily illustrated in an "unrolled" Schwann cell (Fig. 11 *A*). The continuous channel network (light gray) borders the compact myelin domains (dark gray) and consists of the outer loop, paranodal channels, the inner loop and the Schmidt-Lanterman incisures. The data in this study demonstrates that E-cadherin sites (black) have a restricted distribution within the cytoplasmic network. Diagrammed in situ (Fig. 11 *B, bottom*), E-cadherin loci become aligned in contiguous cytoplasmic wraps, thus forming extended junctional complexes. This is most evident in the paranodal channel (Fig. 11 *B, top*) where two helically oriented junctional complexes (black) are depicted. Note that the orientation of

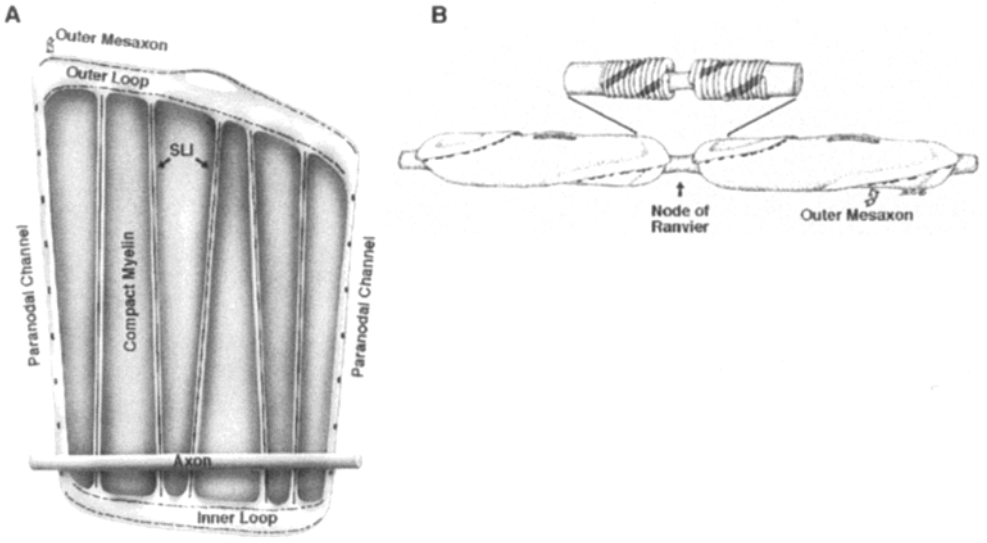

Figure 11. Model for the distribution of E-cadherin adherence sites in an "unrolled" Schwann cell, in the paranodal channels and in a native Schwann cell. (*A*) In an unrolled Schwann cell, E-cadherin adherence sites are found in regions which form the outer boundaries of the cell. These include the outer mesaxon, the outer loop, the inner loop and the paranodal channel. E-cadherin adherence sites are also found in the internal portion of the cell in the Schmidt-Lanterman incisures. Thus, E-cadherin loci are restricted to a cytoplasmic network which sequesters compact myelin into discrete domains. (*B, bottom*). In a Schwann cell in its native ("rolled") conformation, E-cadherin adherence sites become aligned with each other, allowing the formation of an extensive series of transcytoplasmic densities which contribute to the overall stability of the cell. The location of the E-cadherin adherence sites in the outer mesaxon suggests that the outer mesaxon helically wraps around the cell and its orientation continues in register in the adjacent cell. (*B, top*). In paranodal channels stripped of their myelin, E-cadherin containing densities form two helically oriented complexes of transcytoplasmic densities in each paranode.

these complexes is in register across the node of Ranvier. This model for the organization of paranodal junctions is based on confocal and immuno-electron microscopy (this study), and serial electron microscopy (Harkin, 1964). In the outer loop, E-cadherin loci are helically placed, which gives the impression that the outer mesaxon twists along the length of the internode (Fig. 11 *B, lower*) Attachment sites at the outer mesaxon have been previously noted (Bunge et al., 1989), and it is of great interest that freeze–fracture studies reveal extensive linear arrays of particles on the P face at the mesaxonal border (Peters et al., 1991). Some of these particles may, in fact, correspond to E-cadherin loci.

We can speculate that adherens junctions in the Schwann cell may assist in compensatory mechanisms during the stretching and contraction of peripheral nerve. Mechanical stresses on nerve fibers may perhaps be accommodated by changing the degree of coiling of the helical E-cadherin tracts. In this regard, it should be noted that expansion and contraction of Schmidt-Lanterman incisures have been observed in situ (Singer and Bryant, 1969). The alignment of the tracts in the outer loop and mesaxon from one internode to the next suggests that responses may even be coordinated along the entire length of an individual fiber. The adherens junctions in the paranodes may locally supplement the response by maintaining a constant length at the node of Ranvier. This is important since it is generally believed that to ensure efficient saltatory conduction, sodium channels in the nodal axon must be sequestered within relatively non-variant membranous area (Rosenbluth, 1988; Joe and Angelides, 1992).

Autotypic adherens junctions in the Schwann cell may have evolved to mediate rapid intracellular communication which would bypass signaling around the spiral turns. Recent studies have demonstrated that some components of adherens junctions, notably, β-catenin and plakoglobin, are homologues of the Drosophila protein, armadillo, which has been shown to be involved in signal transduction pathways (Nusse and Varmus, 1992). The fact that Schwann cell junctions completely straddle the cytoplasm suits their putative function as efficient signal transducers, and is consistent with the notion that adherens junctions are involved in cellular communication (Gumbiner, 1993; Peifer, 1993).

E-Cadherin may also organize and polarize Schwann cell plasma membrane proteins and other junctional components. Past studies have indicated that adherens junctions and E-cadherin are involved in tissue morphogenesis (Wheelock and Jensen, 1992) and are integral to the maintenance of a polarized epithelium. In addition, E-cadherin seems to act as an organizer of other cell adhesion molecules, and is involved in long-term assembly of the plasma membrane. In the Schwann cell plasma membrane, there is, in effect, a sharply polarized distribution of the two bona fide adhesion molecules characterized in these cells to date: P_0, a member of the Ig superfamily, is restricted to compact myelin, and E-cadherin is restricted to the channel network. The plasma membrane of the Schwann cell actually has four contact sites, three of which have been described as authentic junctions. These include adherens junctions (this paper); tight junctions, (also termed zonula occludens; Mugnaini and Schnapp, 1974; Schnapp and Mugnaini, 1978; Peters et al., 1991); and axoglial junctions, which bridge the paranodal channel and the axonal membrane. The fourth contact site is compact myelin which is a vast planar junction. These junctions are stereotypically organized within the Schwann cell, particularly within the paranodal loops. In fact E-cadherin may play an integral role in establishing Schwann cell polarity in a manner that is analogous to, but certainly distinct from, that in other epithelial cells.

The formation of autotypic junctions must have a crucial role in myelinogenesis. During development of the sheath,

there is both circumferential deposition of myelin lamellae and longitudinal expansion of Schwann cell membrane that proceeds in parallel with the lengthening of the axonal fiber (Webster, 1971). In the establishment of the node of Ranvier, each successive paranodal turn must guide itself around the adjacent channel segment to establish axonal contact. Junctions in the paranodes, Schmidt-Lanterman incisures and outer loops probably stabilize subsequent wraps of myelin as the sheath enlarges. As each turn is completed, newly formed plaques may link with those from previous wraps and, thus, result in contiguously arranged transcytoplasmic junctions. As the myelin sheath forms, E-cadherin mediated adhesive bonds may be continually established, dissociated, and re-established. This activity is likely to depend on interactions between E-cadherin and the actin cytoskeleton, and it is worth noting in this regard that F-actin is localized in peripheral nerve in a labeling pattern that is extraordinarily congruent to E-cadherin distribution (this study; see also Trapp et al., 1989). The adhesive interplay between noncompacted membranes required during myelinogenesis may be analogous to that found in epithelial compaction in which E-cadherin seems to be the major mediator of adhesion (Fleming and Johnson, 1988). During the compaction process, it is thought that E-cadherin induces submembranous, transient changes that are labile and cell contact dependent. Thus, E-cadherin is a good candidate for directing the transient alterations in adhesivity which are likely to be involved in the sequential laying down of the myelin spiral.

In the mature sheath the transcytoplasmic plaques may act as a scaffolding, and perhaps serve to maintain a minimum cytoplasmic width. The absence of a cytoplasmic undercoating at the inner mesaxon may be indicative of more labile membrane–membrane interactions, although there is no direct experimental evidence to support this at present. The relative lability of this interaction would be consistent with one model for myelin membrane deposition that predicts that the myelin sheath enlarges by addition of membrane at the inner loop concurrent with the movement of the inner loop around the axon (Bunge et al., 1989). However, addition of myelin components at the inner loop is not likely to be the only mechanism by which myelin components are deposited in the sheath inasmuch as others have demonstrated that the paranodal and outer loops are also sites of vigorous myelin-related synthetic activity (Gould and Sinatra, 1981; Griffiths et al., 1989), and probable membrane deposition.

In conclusion, E-cadherin is a major adhesion protein in peripheral nerve Schwann cells and is unusual in that it mediates adhesion between membranes synthesized by a single cell. E-cadherin localizes to unique adhesion specializations, now identified as autotypic adherens junctions, that are restricted to subdomains within the noncompacted regions. The junctional complexes may be important stabilization sites in myelination and may mediate rapid signaling across cytoplasmic compartments, which suggests specialized functions in addition to those required for myelinogenesis. Our findings also indicate that the orientations of cytoplasmic networks in Schwann cells are in register across adjacent internodes and this implies that contiguous Schwann cells may have the capacity to act in concert with each other as part of a globally interactive unit. Most importantly, because E-cadherin is fundamentally involved in cellular organization in other cell systems, our data allows us to adduce that E-cadherin may have a similar role in organizing the polarized distributions of Schwann cell proteins, such as P_0 and other components of the myelin sheath. Finally the localization of E-cadherin at the border of each compact myelin domain, taken together with the known susceptibility of this molecule to proteolyze under certain conditions, suggests that failure of E-cadherin mediated adhesion may be one means by which demyelination may proceed in certain pathological states in peripheral nerve.

The authors thank Ms. Jill Gregory for artwork, and Lawrence Shapiro and Drs. Wayne Hendrickson, Harry Webster, Jack Rosenbluth, Barry Gumbiner, and Mary Bunge for helpful discussions. This is manuscript number 172 from the Brookdale Center for Molecular Biology.

This investigation was supported by National Institutes of Health grant NS20147 and by a pilot grant to D. R. Colman and a fellowship to A. M. Fannon (FA 1024-A-1) from the National Multiple Sclerosis Society. Initial support was also provided by a fellowship to A. M. Fannon from the Human Frontier Science Program Organization. V. L. Friedrich was supported by National Institutes of Health grant NS 29056. P. J. Brophy acknowledges support from the Multiple Sclerosis Societies of Great Britain.

Received for publication 13 August 1994 and in revised form 29 December 1994.

References

Behrens, J., M. M. Mareel, R. F. Van, and W. Birchmeier. 1989. Dissecting tumor cell invasion: epithelial cells acquire invasive properties after the loss of uvomorulin-mediated cell–cell adhesion. *J. Cell Biol.* 108:2435–2447.

Bergoffen, J., S. S. Scherer, S. Wang, M. Oronzi Scott, L. J. Bone, D. L. Paul, K. Chen, M. W. Lensch, P. F. Chance, and K. H. Fishbeck. 1993. Connexin mutations in X-linked Charcot-Marie-Tooth disease. *Science (Wash. DC).* 22:2039–2042.

Berndorff, D., R. Gessner, B. Kreft, N. Schnoy A. M. Lajouspetter N. Loch, W. Reutter, M. Hortsch, and R. Tauber. 1994. Liver-intestine cadherin: molecular cloning and characterization of a novel Ca^{2+}-dependent cell adhesion molecule expressed in liver and intestine. *J. Cell Biol.* 123:1353–1369.

Blank, W. F., M. B. Bunge, and R. P. Bunge. 1974 The sensitivity of the myelin sheath particularly the Schwann cell-axolemma junction, to lowered calcium levels in cultured sensory ganglia. *Brain Res.* 67:503–518.

Boller K., D. Vestweber, and R. Kemler. 1985. Cell-adhesion molecule uvomorulin is localized in the intermediate junctions of adult intestinal epithelial cells. *J. Cell Biol.* 100:327–332.

Bunge, R. P., M. B. Bunge, and M. Bates. 1989. Movements of the Schwann cell nucleus implicate progression of the inner (axon-related) Schwann cell process during myelination. *J. Cell Biol.* 109:273–284.

Doyle, J. P., and D. R. Colman. 1993. Glial-neuron interaction and the regulation of myelin formation. *Curr. Opin. Cell Biol.* 5:779–785.

D'Urso D., P. J. Brophy, S. M. Staugaitis, C. S. Gillespie, A. B. Frey, J. G. Stempak, and D. R. Colman. 1990. Protein zero of peripheral nerve myelin: biosynthesis membrane insertion, and evidence for homotypic interaction. *Neuron.* 4:449–460.

Einheber S., T. A. Milner, F. Giancotti and J. L. Salzer. 1993. Axonal regulation of Schwann cell integrin expression suggests a role for alpha 6 beta 4 in myelination. *J. Cell Biol.* 123:1223–1235.

Filbin, M., F. S. Walsh, B. D. Trapp, J. A. Pizzy, and G. I. Tennekoon. 1990. Role of myelin P_0 protein as a homophilic adhesion molecule. *Nature (Lond.).* 34:871–872.

Fleming T. P., and M. H. Johnson. 1988. From egg to epithelium. *Annu. Rev. Cell Biol.* 4:459–485.

Geiger, B., and O. Ayalon. 1992. Cadherins. *Annu. Rev. Cell Biol.* 8:307–332.

Geiger, B., and D. Ginsberg. 1991. The cytoplasmic domain of adherens-type junctions. *Cell Motil. & Cytoskeleton.* 20:1–6.

Ghabriel, M. N., and G. Allt. 1981. Incisures of Schmidt-Lanterman. *Prog. Neurobiol.* 17:25–58.

Gillespie, C. S., D. L. Sherman, G. E. Blair, and P. J. Brophy. 1994. Periaxin, a novel protein of myelinating Schwann cells with a possible role in axonal ensheathment. *Neuron.* 12:497–508.

Gould, R. M., and R. S. Sinatra. 1981. Internodal distribution of phosphatidylcholine biosynthetic activity in teased peripheral nerve fibres: an autoradiographic study. *J. Neurocytol.* 10:161–167.

Griffiths J. R., L. S. Mitchell, K. McPhilemy, S. Morrison, E. Kyriakides, and J. A. Barrie. 1989. Expression of myelin protein genes in Schwann cells. *J. Neurocytol* 18:345–352.

Grunwald, G. B. 1993. The structural and functional analysis of cadherin calcium-dependent cell adhesion molecules. *Curr. Opin. Cell Biol.* 5:797–805.

Gumbiner B., and K. Simons. 1987. The role of uvomorulin in the formation of epithelial occluding junctions. *Ciba Found. Symp.* 125:168–186.

Gumbiner, B. M. 1993. Proteins associated with the cytoplasmic surface of adhesion molecules. *Neuron.* 11:551–564.

Hall, S. M., and P. L. Williams. 1970. Studies on the 'incisures' of Schmidt and Lanterman. *J. Cell Sci.* 6:767–791.

Harkin, J. C. 1964. A series of desmosomal attachments in the Schwann sheath of myelinated mammalian nerves. *Z. Zellforsch. Mikrosk. Anat.* 64:189–195.

Harlow, E., and D. Lane. 1988. Antibodies: A Laboratory Manual. Cold Spring Harbor Laboratory, Cold Spring Harbor, NY. 726 pp.

Hinck, L., I. S. Näthke, J. Papkoff, and W. J. Nelson. 1994. Dynamics of cadherin/catenin complex formation: Novel protein interactions and pathways of complex assembly. *J. Cell Biol.* 125:1327–1340.

Hirano S., N. Kimoto, Y. Shimoyama, S. Hirohashi, and M. Takeichi. 1992. Identification of a neural alpha-catenin as a key regulator of cadherin function and multicellular organization. *Cell.* 70:293–301.

Joe E. H., and K. Angelides. 1992. Clustering of voltage-dependent sodium channels on axons depends on Schwann cell contact. *Nature (Lond.).* 356:333–335.

Kintner, C. 1992. Regulation of embryonic cell adhesion by the cadherin cytoplasmic domain. *Cell.* 69:225–236.

Kordeli, E., J. Davis, B. Trapp, and V. Bennett. 1990. An isoform of ankyrin is localized at Nodes of Ranvier in myelinated axons of central and peripheral nerves. *J. Cell Biol.* 11:1341–1352.

Le Bivic, A., Y. Sambuy, K. Mostov, and E. Rodriguez-Boulan. 1990. Vectorial targeting of an endogenous apical membrane sialoglycoprotein and uvomorulin in MDCK cells. *J. Cell Biol.* 10:1533–1539.

Lee V. M.-Y., M. J. Carden, W. W. Schlaepfer, and J. O. Trojanowski. 1987. Monoclonal antibodies distinguish several differentially phosphorylated states of the two largest rat neurofilament subunits (NF-H and NF-M) and demonstrate their existence in the normal nervous system of the adult rat. *J. Neurosci.* 7:3474–3488.

Magee, A. I., and R. S. Buxton. 1991. Transmembrane molecular assemblies regulated by the greater cadherin family. *Curr. Opin. Cell Biol.* 3:854–861.

Mugnaini, E., and B Schnapp. 1974. Possible role of zonula occludens of the myelin sheath in demyelinating conditions. *Nature (Lond.).* 251:725–727.

Nagafuchi, A., and M. Takeichi. 1988. Cell binding function of E-cadherin is regulated by the cytoplasmic domain. *EMBO (Eur. Mol. Biol. Organ.) J.* 7:3697–3684.

Nagafuchi, A., Y. Shirayoshi, K. Okazari, K. Yasuda, and M. Takeichi. 1987. Transformation of cell adhesion properties by exogenously introduced E cadherin cDNA. *Nature (Lond.).* 329:341–343.

Näthke, I. S., L. Hinck, J. R. Swedlow, J. Papkoff and W. J. Nelson. 1994. Defining interactions and distributions of cadherin and catenin complexes in polarized epithelial cells. *J. Cell Biol.* 125:1341–1352.

Nusse, R., and H. E. Varmus. 1992. Wnt genes. *Cell.* 69:1073–1087.

Ozawa, M., H. Baribault, and R. Kemler. 1989. The cytoplasmic domain of the cell adhesion molecule uvomorulin associates with three independent proteins structurally related in different species. *EMBO (Eur. Mol. Biol. Organ.) J.* 8:1711–1717.

Peifer, M. 1993. The product of the drosophila segment polarity gene armadillo is part of a multi-protein complex resembling the vertebrate adherens junction. *J. Cell Sci.* 105:993–1000.

Peters, A., S. L. Palay, and H. deF. Webster. 1991. The Fine Structure of the Nervous System: Neurons and their Supporting Cells. Oxford University Press, New York. 494 pp.

Rosenbluth J. 1988. Role of glial cells in the differentiation and function of myelinated axons. *Int. J. Dev. Neurosci.* 6:3–24.

Schnapp, B., and E. Mugnaini. 1978. Membrane architecture of myelinated fibers as seen by freeze-fracture. *In* Physiology and Pathobiology of Axons. S. Waxman, editor. Raven Press, New York. 83–123.

Shimamura, K., T. Takahashi, and M. Takeichi. 1992. E-cadherin expression in a particular subset of sensory neurons. *Dev. Biol.* 152:242–254.

Shirayoshi, Y., A. Nose, K. Iwasaki, and M. Takeichi. 1986. N-linked oligosaccharides are not involved in the function of cell-cell binding glycoprotein E-cadherin. *Cell Struct. Func.* 11:245–252.

Singer M., and S. Bryant. 1969. Movements in the myelin Schwann sheath of the vertebrate axon. *Nature (Lond.).* 221:1148–1150.

Takeichi, M. 1991. Cadherin cell adhesion receptors as a morphogenetic regulator. *Science (Wash. DC).* 251:1451–1455.

Trapp, B. D., S. B. Andrews, A. Wong, M. O'Connell, and J. W. Griffin. 1989. Co-localization of the myelin-associated glycoprotein and the microfilament components, F-actin and spectrin, in Schwann cells of myelinated nerve fibres. *J. Neurocytol.* 18:47–60.

Uchiyama N., M. Hasegawa, T. Yamashima, J. Yamashita, K. Shimamura, and M. Takeichi, 1994. Immunoelectron microscopic localization of E-cadherin in dorsal root ganglia, dorsal root and dorsal horn of postnatal mice. *J. Neurocytol.* 23:460–468.

Volk, T., and B. Geiger. 1986*a*. A-CAM: a 135-kD receptor of intercellular junctions. I. Immunoelectron microscopic localization and biochemical studies. *J. Cell Biol.* 103:1441–1450.

Volk, T., and B. Geiger. 1986*b*. A-CAM: a 135-kD receptor of intercellular adherens junctions. II. Antibody-mediated modulation of junctions. *J. Cell Biol.* 103:1451–1464.

Webster H. deF. 1971. The geometry of peripheral myelin sheaths during their formation and growth in rat sciatic nerve. *J. Cell Biol.* 48:348–367.

Wheelock M. J., and P. J. Jensen. 1992. Regulation of keratinocyte intercellular junction organization and epidermal morphogenesis by E-cadherin. *J. Cell Biol.* 117:415–425.